JACS
JOURNAL OF THE AMERICAN CHEMICAL SOCIETY

COMMUNICATION

pubs.acs.org/JACS

Pore Formation in Phospholipid Bilayers by Branched-Chain Pyrogallol[4]arenes

Saeedeh Negin,[†] Megan M. Daschbach,[†] Oleg V. Kulikov,[†] Nigam Rath,[†] and George W. Gokel*[,†,‡]

[†]Center for Nanoscience, Departments of Chemistry & Biochemistry and [‡]Biology, University of Missouri - Saint Louis, Saint Louis, Missouri 63121, United States

Supporting Information

ABSTRACT: Pyrogallolarenes are tetrameric macrocycles that form from 1,2,3-trihydroxybenzene and aldehydes under acidic conditions. When 2-ethylbutanal or 2-propylpentanal was so treated, the branched-chain pyrogallolarenes crystallized as nanotubes or bilayers, respectively. When the behavior of each compound was assessed by using the planar bilayer conductance method, pore formation was observed. The properties of the pores were significantly different from each other, probably reflecting different types of pore organization within the membrane.

Calixarenes, resorcinarenes, pyrogallarenes, calixpyrroles, and their numerous variants have become, arguably, the dominant supramolecular receptor scaffold.[1] Applications are as diverse as cation binding[2] and as sensor components for urinalysis.[3] Aggregates have also served as "nanoflasks" for physical organic chemical studies[4] and as molecular capsules that enclose guests.[5]

Pyrogallol[4]arenes are compounds formed by the acid-catalyzed condensation of pyrogallol with an aldehyde.[6] Most, but certainly not all, of the characterization of pyrogallolarenes has been done by using solid state analytical methods, particularly X-ray crystallography. Mattay,[7] Atwood,[8] and Rissanen[9] and their co-workers have been leaders in establishing structures, which are typically obtained from compounds isolated in the "cone" or "*rccc*" conformation. The crystal structures reveal bilayer, capsule,[10] and nanotube assemblies.[11,12] The ability of compounds in this family to exhibit membrane activity is becoming increasingly apparent.[13−15]

We have been particularly interested in the dynamic properties of these compounds, whether they form bilayers or capsules[16] in the solid state. In either case, the H-bond network[17] involves a "head-to-head" organization.[18] In the hexameric capsular form, replacement of H-bonds by coordinated copper led to a metallorganic nanocapsule[19] that transported ions through a bilayer and showed a 2.4:1 selectivity for K^+ over Cl^-.[14] Certain pyrogallol[4]arenes can insert into a phospholipid bilayer and form ion-conducting pores.[15] When the pyrogallol[4]arene side chains were 3-pentyl (diethylmethyl), unique, interlocked nanotubes were formed.[20] Nanotubes formed from cyclic peptides[21] such as those reported by Ghadiri, Granja, and co-workers[22] are known to form ion-conducting channels in bilayers.[23] We now report the formation of channels from two branched-chain pyrogallol[4]arenes that crystallize either as nanotubes or as bilayers and form pores by apparently different mechanisms.

Pyrogallol (1,2,3-trihydroxybenzene) was heated under reflux in a mixture of HCl and EtOH in the presence of either $(CH_3CH_2)_2CHCHO$ or $(CH_3CH_2CH_2)_2CHCHO$. The resulting pyrogallolarenes, **1** and **2**, crystallized as a nanotube $[(\mathbf{1}_6)_n]$[20] or a bilayer $(\mathbf{2}_n)$.[24] The structures of the monomers are illustrated as **1** and **2**.

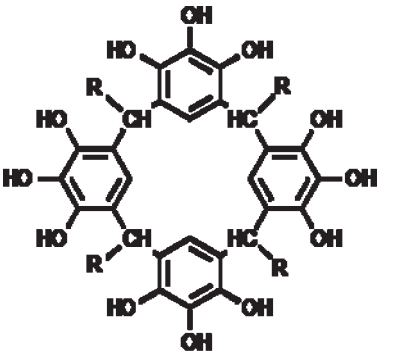

1, R = $CH(CH_2CH_3)_2$
2, R = $CH(CH_2CH_2CH_3)_2$

The nanotubes $[(\mathbf{1}_6)_n]$ were crystallized either from EtOH/EtOAc or from EtOAc/CH_3CN. We previously reported the structure of the nanotube obtained from EtOH/EtOAc.[20] The sample of $[(\mathbf{1}_6)_n]$ used here crystallized from EtOAc/CH_3CN, and its structure is shown in Figure 1.[24] The previously reported structure of $(\mathbf{1}_6)_n$ has 2 EtOH and 6 H_2O molecules linked within each hexamer. In the present case, the organized solvent within each hexamer includes (on average) 4 EtOAc and 9 CH_3CN molecules. One of the hexameric units that stack to form the nanotube is shown in the upper panel of Figure 1.

Compound **2**, which has 3-heptyl (dipropylmethyl) side chains, crystallized in the bilayer arrangement. While the nanotube arrangement of **1** leads to extended tubular chains of micrometer dimensions,[20] **2** forms a bilayer $(\mathbf{2}_n)$ having a thickness of ~17.6 Å. The lower panel of Figure 1 shows, both in space-filling and stick representations, the head-to-head dimer that is the minimal subunit of the extended bilayer. Although the bilayer arrangement is the most typical solid-state motif for pyrogallolarenes, the organization of **1** into nanotubes is fostered by the interlocking of the ethyl side chains. We attempted numerous crystallizations of 4-heptyl-Pg (**2**) in the hope of

Received: September 30, 2010
Published: February 22, 2011

dx.doi.org/10.1021/ja1085645 | *J. Am. Chem. Soc.* 2011, 133, 3234–3237

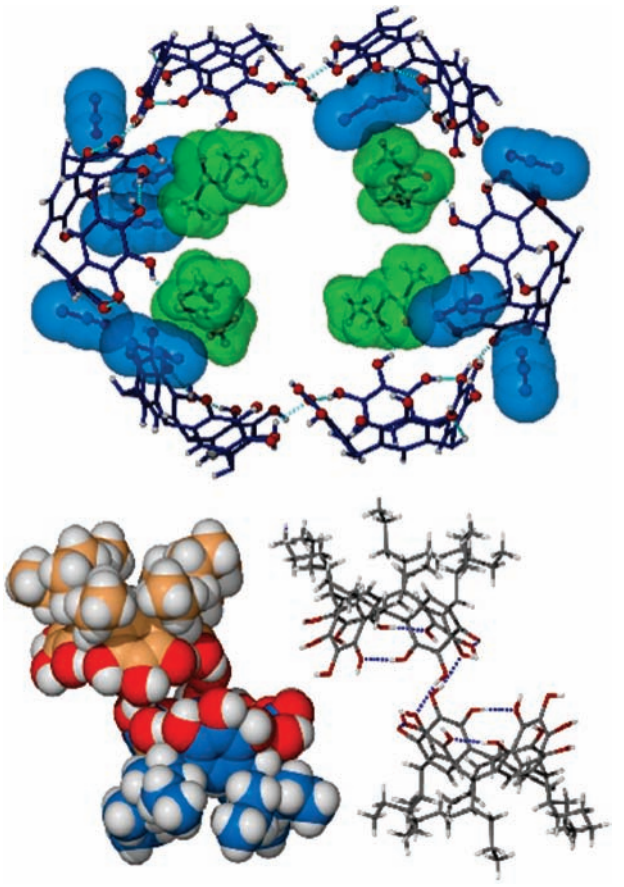

Figure 1. (Top) A single hexameric "doughnut" unit of the $(\mathbf{1}_6)_n$ nanotube crystallized from EtOAc/CH_3CN. (Bottom) Solid-state bilayer structure of **2** showing a single dimer unit in both space-filling and stick representations.

forming nanotubes. Instead, X-ray crystallography revealed only the "bilayer" arrangement for **2** (i.e., $\mathbf{2}_n$, see Figure 1, above). The lateral interlocking of the side chain ethyl groups in $\mathbf{1}_6$ or the resultant nanotubes ($(\mathbf{1}_6)_n$) is not possible with the larger propyl groups of **2**. Not only do $(\mathbf{1}_6)_n$ and $\mathbf{2}_n$ differ in their crystallization behavior, but their ability to form pores in the bilayer is also distinct.

We examined the behavior of both $(\mathbf{1}_6)_n$ and $\mathbf{2}_n$ in an asolectin (from soybean) bilayer membrane by using a planar bilayer conductance apparatus.[25] Each chamber of the instrument contained 450 mM aqueous KCl in 10 mM HEPES buffer at pH 7. 3-Pentyl-Pg, $(\mathbf{1}_6)_n$ was dissolved in dimethylsulfoxide (DMSO) and added to the cis chamber to a final concentration of 7 μM. The same conditions were used for **2**. Figure 2 shows planar bilayer conductance data for compounds **1** (upper trace) and **2**. The traces are directly comparable: the current and time scales are the same for both recordings although the applied potentials differ (**1**, 50 mV; **2**, 60 mV). A comparison of the two ~200 s recordings shown for **1** and **2** reveals the more dynamic behavior of **2**. Dashed lines have been superimposed on the traces to correlate open states. Two states dominate the conductance behavior of **1**, i.e., 460 pS and 1080 pS. We exclude very short duration conductance states that may be interpreted as noise spikes. The lower trace (**2**) shows at least five independent states (66 pS, 233 pS, 500 pS, 566 pS, and 766 pS) as well as apparent multiple-channel openings. The obvious differences between the behavior of **1** and **2** in these traces are representative of the full recordings for both compounds.

We noted above that **1** crystallizes as a cyclic hexamer that forms nanotubes by stacking one hexamer upon another. We have interpreted the behavior of **1** in the bilayer in terms of a hexameric array of Pgs. Two hexameric macrocycles stacked one upon the other within the bilayer would form a channel. When these two stacked hexamers slide laterally with respect to each other, they would gate, i.e., open and close, the channel. The integrity of the cyclic hexamer was challenged by conducting the planar bilayer experiment on a sample of $\mathbf{1}_n$ dissolved in DMSO and maintained at ambient temperature for 24 h prior to the conductance experiment. Substantially the same results as shown in Figure 2 were obtained.

The longest open state apparent at the left of the upper trace has a conductance twice that of the states apparent at the right. If a protein channel were under study, one might interpret the higher conductance state to reflect two channel openings. It may be possible that two channels open and close at precisely the same time, but this seems unlikely. If two hexameric pores (~460 pS) stacked vertically within the bilayer align and interact, the result would be a twinned pore. The "top" and "bottom" pairs (structures such as ∞) could then slide laterally with respect to each other to form a 1080 pS conductance state with coordinated opening behavior. The 3-pentyl side chains of **1** are known to interlock laterally in the solid state as do the cogs of a gear.[20]

The ion transport behavior of **2**, shown in Figure 2, is superficially similar in some respects to that recorded for **1**. There are three key differences. First, the behavior of **2** in the bilayer is more dynamic and more varied than that observed for **1**. The dotted lines in Figure 2 identify eight conductance states. Second, the two longer duration states that appear to resemble those observed for **1** have conductances of ~233 pS and ~566 pS compared to ~460 pS and ~1080 pS. Third, the longer duration states for **2** show multiple, superimposed open states.

As shown in Figure 1, **2** crystallizes as a bilayer, and we have thus far found no solid-state evidence for any special longitudinal or lateral organization for this compound. In previous work[8] with linear alkyl-chained Pgs, we have observed well-behaved oligomeric pores that form in the bilayer. Although **2** possesses eight propyl side chains, the pores it forms are clearly very dynamic, and multiple oligomers must be present. We note that *tetra*(*n*-propyl)pyrogallol[4]arene disrupted a planar bilayer, but only spiking behavior could be discerned. In the case of **2**, the abundance of chains may facilitate side-chain contacts and thus oligomerization, but the shortness of the chains and the lack of any obvious organizational mechanism such as found in **1**, prevents the formation of dominant or preponderant states. Presumably, lateral side-chain interactions in **2** lead to pore formation within the bilayer. Absent the special stabilization apparent in the solid-state structure of **1**, **2** forms far more dynamic assemblies. The assemblies of $\mathbf{2}_n$ will have numbers of Pgs similar to those in $\mathbf{1}_6$, and some similarity in open-state conductances is to be expected.

Using the data obtained from the planar bilayer experiments (i.e., 460 pS), we used the Hille equation[26] to calculate a pore size of ~17 Å. This corresponds well with the size of the individual hexameric units of $(\mathbf{1}_6)$ that link together to form the nanotube (internal dimensions: 18 Å × 20 Å).[20] On the basis of the sizes apparent in the solid-state structure, we estimate that the thickness of each individual disk is ~12 Å. Two such units, when stacked, span ~24 Å. The insulator regime of a bilayer is typically

dx.doi.org/10.1021/ja1085645 |*J. Am. Chem. Soc.* 2011, 133, 3234–3237

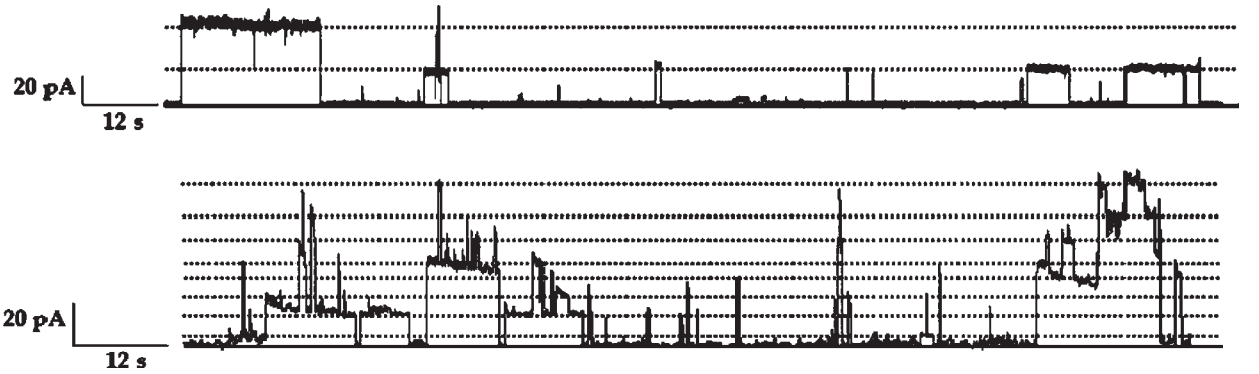

Figure 2. Planar bilayer conductance traces for $(\mathbf{1}_6)_n$ (top, 50 mV) and $\mathbf{2}_n$ (bottom, 60 mV). Current is indicated on the ordinate and duration on the abscissa (see scales).

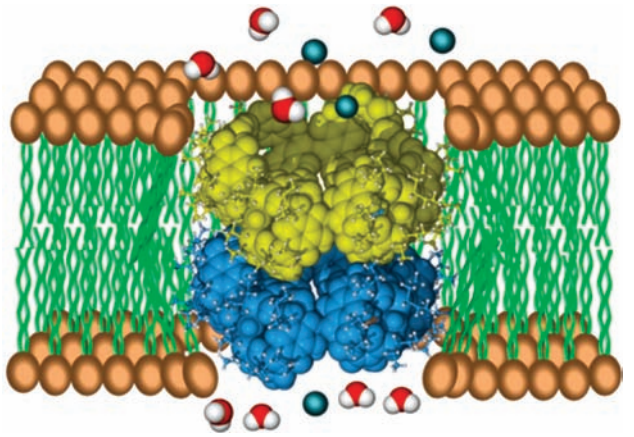

Figure 3. Possible pore formation mechanism for $\mathbf{1}_6$.

stated to be ~30 Å thick. It is known, however, that membranes typically narrow at the site of pore formation[27] so two units, spanning 24 Å is potentially a more reasonable model.

The formation of nanotubes from **1** involves an extensive H-bond network that connects the six pyrogallol[4]arenes into the macrocyclic hexamer. Solvent also is linked between individual monomers. Stacking of the hexamers is fostered by solvent exclusion and the interlocking of side-chain ethyl groups as noted previously.[20] We speculate that the crystalline nanotube dissociates in DMSO into individual disk units. These hexamers ($\mathbf{1}_6$) retain their organization owing primarily to the network of H-bonds involving the pyrogallol hydroxyl groups. The hexamers penetrate the bilayer and then stack within the membrane. This interaction is fostered by solvent exclusion and contacts between the pentyl side chains and the fatty acyl chains. Lateral motion of the pair (or triplet) of $\mathbf{1}_6$ with respect to each other would permit the passage or restraint of ions (i.e. open, close), and when open, the pore size corresponds well with the observed internal diameter of nanotube $(\mathbf{1}_6)_n$. This possible mechanism is shown schematically in Figure 3.

As noted above, similar conductance behavior was observed for **1** even after standing in DMSO solution for 24 h suggesting the integrity of the putative hexamer assembly. In order to obtain additional information on the self-assembly of **1** and to confirm the difference in behavior between **1** and **2**, we cospread it on the Langmuir trough with dipalmitoylphosphatidyl choline (DPPC).[28] When two amphiphiles are cospread, absent unexpected interactions, the surface pressure−area isotherms will appear at proportional values between those determined for the individual amphiphiles.[28,29] The behavior of **2** alone was as expected as were most mixtures of **1** and DPPC. However, at high concentrations of **1** relative to DPPC, a discontinuity was apparent. The anomaly was interpreted as "holes" in the monolayer that corresponded in size to the formation of cyclic hexamers of **1**. An analysis of void areas corresponded to the area within the hexameric pore. The experimental results are detailed in Supporting Information. Further, Brewster angle microscopy showed a continuous surface for mixtures of DPPC and **1**. This contrasts with the extensive surface organization apparent for **1** alone on the surface of the Langmuir trough.[20]

The pores formed from $\mathbf{2}_n$ clearly differ from those formed by $\mathbf{1}_n$ and there is currently no evidence that they can form a similar tube arrangement. It therefore seems reasonable to assume that the mechanisms of pore formation by $(\mathbf{1}_6)_n$ and $\mathbf{2}_n$ differ. The stacked hexamer mechanism for **1** may seem implausible, but the formation of pores from various stacked monomers has been proposed in several contexts and appears at least credible.[21−23,30] The solid-state and the membrane phases are obviously different, but the lipid chains in the latter provide some of the same organizational forces present in a solid. Studies to confirm the stacking hypothesis for $\mathbf{1}_6$ are currently underway.

■ ASSOCIATED CONTENT

Supporting Information. Experimental procedures, instrument information, and a detailed analysis of the Langmuir trough work. This material is available free of charge via the Internet at http://pubs.acs.org.

■ AUTHOR INFORMATION

Corresponding Author
gokelg@umsl.edu

■ ACKNOWLEDGMENT

We thank the NSF (CHE-0957535) for a grant that supported this work.

■ REFERENCES

(1) (a) Gutsche, C. D. *Calixarenes Revisited*; Royal Society of Chemistry: Cambridge, 1998; Vol. 6. (b) *Calixarenes in Action*; Mandolini, L., Ungaro, R., Eds.; World Scientific Publishing Company: Hackensack, NJ, 2000. (c) Gutsche, C. D. *Calixarenes: An Introduction*

(Monographs in Supramolecular Chemistry), 2nd ed.; Royal Society of Chemistry: Cambridge, UK, 2008. (d) Sliwa, W.; Kozlowski, C. *Calixarenes and Resorcinarenes: Synthesis, Properties, and Applications*; Wiley-VCH, Verlag GmbH & Co.: Weinheim, 2009.

(2) Arduini, A.; Casnati, A.; Pochini, A.; Ungaro, R. *Curr. Opin. Chem. Biol.* **1997**, *1*, 467–474.

(3) Nikolelis, D. P.; Psaroudakis, N.; Ferderigos, N. *Anal. Chem.* **2005**, *77*, 3217–3221.

(4) (b) Amrhein, P.; Wash, P. L.; Shivanyuk, A.; Rebek, J., Jr. *Org. Lett.* **2002**, *4*, 319–321. (a) Shivanyuk, A.; Rebek, J. *Proc. Natl. Acad. Sci. U.S.A.* **2001**, *98*, 7662–7665.

(5) Atwood, J. L.; Szumna, A. *J. Am. Chem. Soc.* **2002**, *124*, 10646–10647.

(6) Haworth, R. D.; Lamberton, A. H. *J. Chem. Soc.* **1946**, 1003–1005.

(7) Gerkensmeier, T.; Agena, C.; Iwanek, W.; Frohlich, R.; Kotilad, S.; Nather, C.; Mattay, J. *Z. Naturforsch.* **2001**, *56*, 1063–1073.

(8) Atwood, J. L.; Barbour, L. J.; Jerga, A. *Chem. Commun.* **2001**, 2376–2377.

(9) Mansikkamaki, H.; Nissinen, M.; Rissanen, K. *Angew. Chem., Int. Ed.* **2004**, *43*, 1243–1246.

(10) Gerkensmeier, T.; Iwanek, W.; Agena, C.; Fröhlich, R.; Kotila, S.; Näther, C.; Mattay, J. *Eur. J. Org. Chem.* **1999**, 2257–2262.

(11) Mansikkamaki, H.; Nissinen, M.; Rissanen, K. *Angew. Chem., Int. Ed.* **2004**, *43*, 1243–1246.

(12) Dalgarno, S. J.; Cave, G. W.; Atwood, J. L. *Angew. Chem., Int. Ed.* **2006**, *45*, 570–574.

(13) (a) Tanaka, Y.; Kobuke, Y.; Sokabe, M. *Angew. Chem., Int. Ed. Engl.* **1995**, *34*, 693–694. (b) Yoshino, N.; Satake, A.; Kobuke, Y. *Angew. Chem., Int. Ed.* **2001**, *40*, 457–459.

(14) Kulikov, O. V.; Li, R.; Gokel, G. W. *Angew. Chem., Int. Ed.* **2009**, *48*, 375–377.

(15) Li, R.; Kulikov, O. V.; Gokel, G. W. *Chem. Commun.* **2009**, 6092–6094.

(16) Kulikov, O. V.; Rath, N. P.; Zhou, D.; Carasel, I. A.; Gokel, G. W. *New J. Chem.* **2009**, *33*, 1563–1569.

(17) Atwood, J. L.; Szumna, A. *J. Am. Chem. Soc.* **2002**, *124*, 10646–10647.

(18) Heaven, M. W.; Cave, G. W.; McKinlay, R. M.; Antesberger, J.; Dalgarno, S. J.; Thallapally, P. K.; Atwood, J. L. *Angew. Chem., Int. Ed.* **2006**, *45*, 6221–6224.

(19) Dalgarno, S. J.; Power, N. P.; Warren, J. E.; Atwood, J. L. *Chem. Commun.* **2008**, 1539–1541.

(20) Kulikov, O. V.; Daschbach, M. M.; Yamnitz, C. R.; Rath, N.; Gokel, G. W. *Chem. Commun.* **2009**, 7497–7499.

(21) Brea, R. J.; Reiriz, C.; Granja, J. R. *Chem. Soc. Rev.* **2010**, *39*, 1448–1456.

(22) Ghadiri, M. R.; Granja, J. R.; Milligan, R. A.; McRee, D. E.; Khazanovich, N. *Nature (London)* **1993**, *366*, 324–327.

(23) Ghadiri, M. R.; Granja, J. R.; Buehler, L. K. *Nature* **1994**, *369*, 301–304.

(24) The crystal coordinates may be found in CCDC 729499; coordinate location, but not the structure, is cited in reference 20.

(25) Warner Instruments, Hamden, CT 06514, United States.

(26) (a) Hille, B. *Ionic Channels of Excitable Membranes*, 3rd ed.; Sinauer Associates: Sunderland, MA, 2001. (b) Smart, O. S.; Breed, J.; Smith, G. R.; Sansom, M. S. P. *Biophys. J.* **1997**, *72*, 1109–1126.

(27) Wi, S.; Kim, C. *J. Phys. Chem. B* **2008**, *112*, 11402–11414.

(28) Haas, H.; Caetano, W.; Borissevitch, G. P.; Tabak, M.; Mosquera Sanchez, M. I.; Olivera, O. N., Jr.; Scalas, E.; Goldmann, M. *Chem. Phys. Lett.* **2001**, *335*, 510–516.

(29) (a) Lee, Y.-L.; Yang, Y.-C.; Shen, Y.-J. *J. Phys. Chem. B* **2005**, *109*, 4662–4667. (b) Gzyl, B.; Paluch, M. *Prog. Colloid Polym. Sci.* **2004**, *123*, 245–250 .

(30) (a) Clark, T. D.; Buehler, L. K.; Ghadiri, M. R. *J. Am. Chem. Soc.* **1998**, *120*, 651. (b) Bhosale, S.; Sisson, A. L.; Sakai, N.; Matile, S. *Org. Biomol. Chem.* **2006**, *4*, 3031. (c) Yang, J.; Dewal, M. B.; Sobransingh, D.; Smith, M. D.; Xu, Y.; Shimizu, L. S. *J. Org. Chem.* **2009**, *74*, 102. (d) Helsel, A. J.; Brown, A. L.; Yamato, K.; Feng, W.; Yuan, L.; Clements, A. J.; Harding, S. V.; Szabo, G.; Shao, Z.; Gong, B. *J. Am. Chem. Soc.* **2008**, *130*, 15784. (e) Yamnitz, C. R.; Negin, S.; Carasel, I. A.; Winter, R. K.; Gokel, G. W. *Chem. Commun.* **2010**, 2838–2840.